

StyTr²: Unbiased Image Style Transfer with Transformers

Yingying Deng, Fan Tang, Xingjia Pan, Weiming Dong *Member, IEEE*, Chongyang Ma, Changsheng Xu, *Fellow, IEEE*

Abstract

The goal of image style transfer is to render an image with artistic features guided by a style reference while maintaining the original content. Due to the locality and spatial invariance in CNNs, it is difficult to extract and maintain the global information of input images. Therefore, traditional neural style transfer methods are usually biased and content leak can be observed by running several times of the style transfer process with the same reference style image. To address this critical issue, we take long-range dependencies of input images into account for unbiased style transfer by proposing a transformer-based approach, namely StyTr². In contrast with visual transformers for other vision tasks, our StyTr² contains two different transformer encoders to generate domain-specific sequences for content and style, respectively. Following the encoders, a multi-layer transformer decoder is adopted to stylize the content sequence according to the style sequence. In addition, we analyze the deficiency of existing positional encoding methods and propose the content-aware positional encoding (CAPE) which is scale-invariant and more suitable for image style transfer task. Qualitative and quantitative experiments demonstrate the effectiveness of the proposed StyTr² compared to state-of-the-art CNN-based and flow-based approaches.

Index Terms

I. INTRODUCTION

Image style transfer is an interesting and practical research topic that can render a content image using another referenced style image. Based on texture synthesis, traditional style transfer methods [1], [2] can generate vivid results but are computationally complex due to the formulation of stroke appearance and painting process. Recently, researchers focus on end-to-end style transfer based on convolutional neural networks (CNNs). Optimization-based style transfer methods [3]–[5] render the input content images with learned style representation iteratively. Following the encoder-transfer-decoder pipeline, arbitrary style transfer networks [6]–[14] are trained by aligning the second-order statistics of content images to style images and can generate stylized results in feed-forward fashion efficiently. However, these methods cannot achieve satisfactory results in some cases due to the limited ability to model the relationship between content and style. To overcome this issue, attention-based methods [15]–[18] apply self-attention mechanism to the transfer module for improved stylization results.

These aforementioned style transfer methods use multi-layer CNNs to learn style and content representations. With the limited receptive fields of convolution layers, CNNs cannot process long-range dependencies. It is hard to obtain global information of input images [19] which is critical for image style transfer task. Figure 1(a) shows the style reconstruction results of CNN-based methods. Features from different layers encode information in different scales while global style representation is hard to merge into the reconstructions. Moreover, An et al. [20] find that content leak occurs when the CNN-based structures are adopted in style transfer task. This phenomenon proves that feature leak exists in the process of feature extraction by CNNs. As depicted in Figure 2(a), the content and style features are biased towards the original input through the encoder and hence lead to feature leak which defaces content and style details in the results. Based on the above phenomenon, ArtFlow [20] adopt a projection flow network to achieve unbiased style transfer. However, due to the weak feature extraction ability of the flow-based model, outstanding stylized results are hard to be obtained.

With the success of Transformer [21] in natural language processing (NLP), the transformer-based architectures have been adopted in various vision tasks. The charm of applying transformer to computer vision lies in that: (1) it has strong representation capability and is free to learn the global information of the inputs through the self-attention mechanism, thus the holistic understanding can be easily obtained by every layer. As shown in Figure 1(b), different layers can be used to generate global promising style reconstruction results with incremental details; (2) the transformer does not contain the inductive biases [22] caused by locality and spatial-invariance, which could avoid content leak in the style transfer task (see Figure 2(b)).

In this work, we aim to get rid of aforementioned problem of CNN-based style transfer structures and propose the unbiased **Style Transfer Transformer** framework, namely StyTr². Different from the original transformer, we design two transformer

Yingying Deng, Weiming Dong and Changsheng Xu are with School of Artificial Intelligence, University of Chinese Academy of Sciences, Beijing, China and NLPR, Institute of Automation, Chinese Academy of Sciences, Beijing, China (e-mail: {dengyingying2017, weiming.dong, changsheng.xu}@ia.ac.cn).

Fan Tang is with Jilin University, Changchun, China (e-mail: tangfan@jlu.edu.cn)

Xingjia Pan is with YouTu Lab, Tencent, Shanghai, China (e-mail: xjia.pan@gmail.com)

Chongyang Ma is with Kuaishou Technology, Beijing, China (e-mail: chongyangma@kuaishou.com).

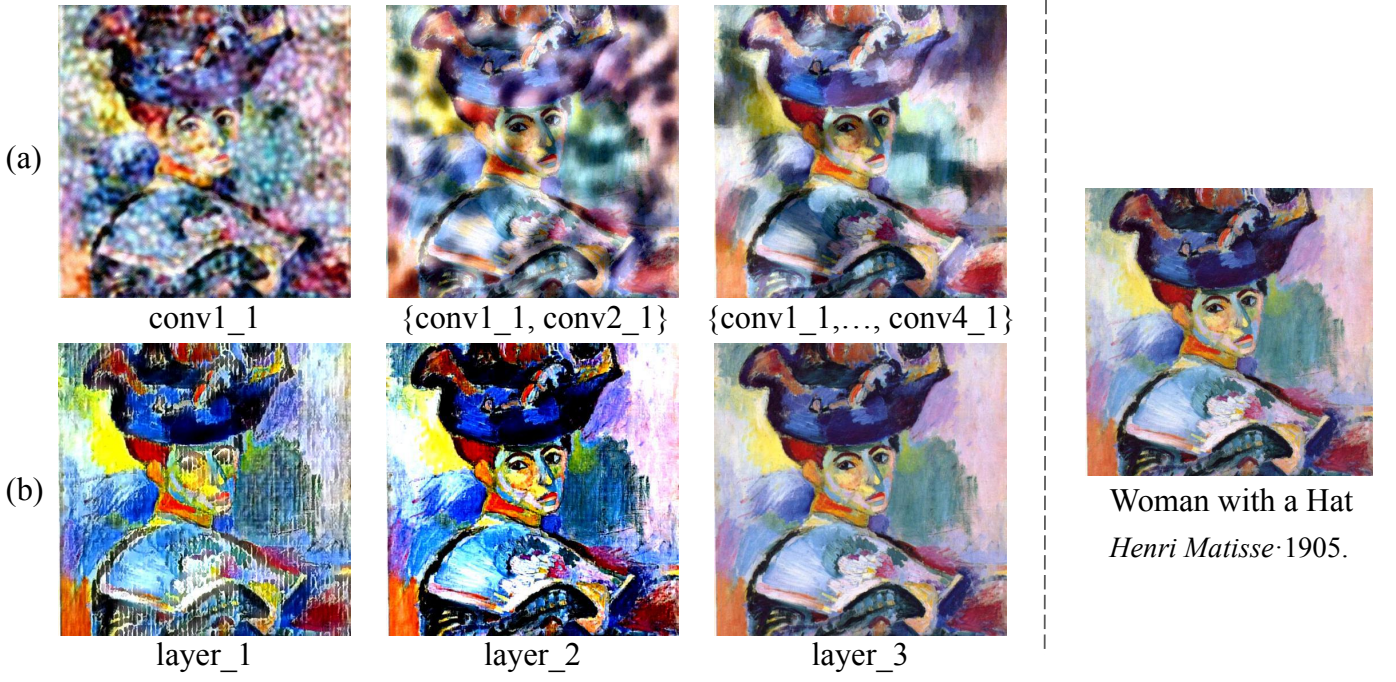


Fig. 1. Comparisons of intermediate layers using the rightmost image as both the content and the style image in a reconstruction task. (a) Image reconstruction results from layers $conv1_1$, $\{conv1_1, conv2_1\}$, $\{conv1_1, conv2_1, conv3_1, conv4_1\}$ of a pretrained VGG network based on Gatys et al. [3]. (b) Feature visualizations of three layers of the transformer decoder.

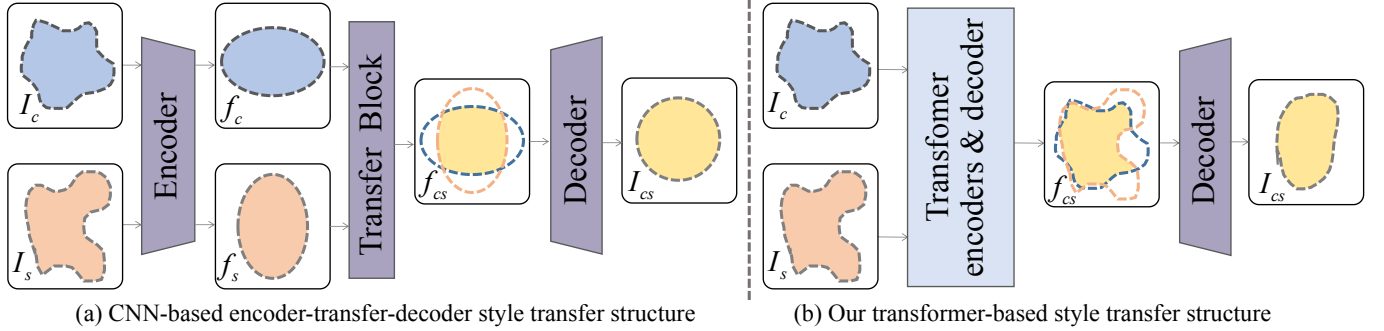


Fig. 2. A comparison of encoder-transfer-decoder style transfer structure and our structure. The CNN-based method could lead to biased style transfer, while the transformer-based method could avoid feature leak and achieve unbiased style transfer.

encoders in our StyTr² framework to obtain domain-specific information. Following the encoders, the transformer decoder is used to progressively generate the output sequences. Furthermore, towards the positional encoding methods that are proposed for NLP, we raise two considerations: (1) different from sentences ordered by logic, the image sequence tokens are associated via semantic information of the image content; (2) for the style transfer task, we aim to generate stylized images of any size. The exponential increase of input images will lead to a dramatic change of positional encoding, which will lead to large position deviation and inferior output quality. In general, a desired positional encoding for vision tasks should be conditioned on input content while be invariant to image scale transformation. Therefore, we propose the content-aware positional encoding (CAPE) which learns the positional encoding based on image semantic features and dynamically expands the position to suit different image sizes.

In summary, our main contributions include: (a) a transformer-based style transfer framework, namely StyTr², to reduce content leak and achieve unbiased stylization; (b) a content-aware positional encoding mechanism which is scale-invariant and suitable for vision generation tasks; and (c) a series of experimental results showing that StyTr² can achieve unbiased stylization and generate outstanding results with clear content structures and vivid style patterns.

II. RELATED WORK

a) Image style transfer.: Gatys et al. [3] find that hierarchical layers in CNNs can be used to extract image content structures and style texture information and proposed an optimization-based method to generate outputs iteratively. Some works [23], [24] adopt an end-to-end model to realize real-time style transfer for one specific style. For more efficient applications, [25], [26]

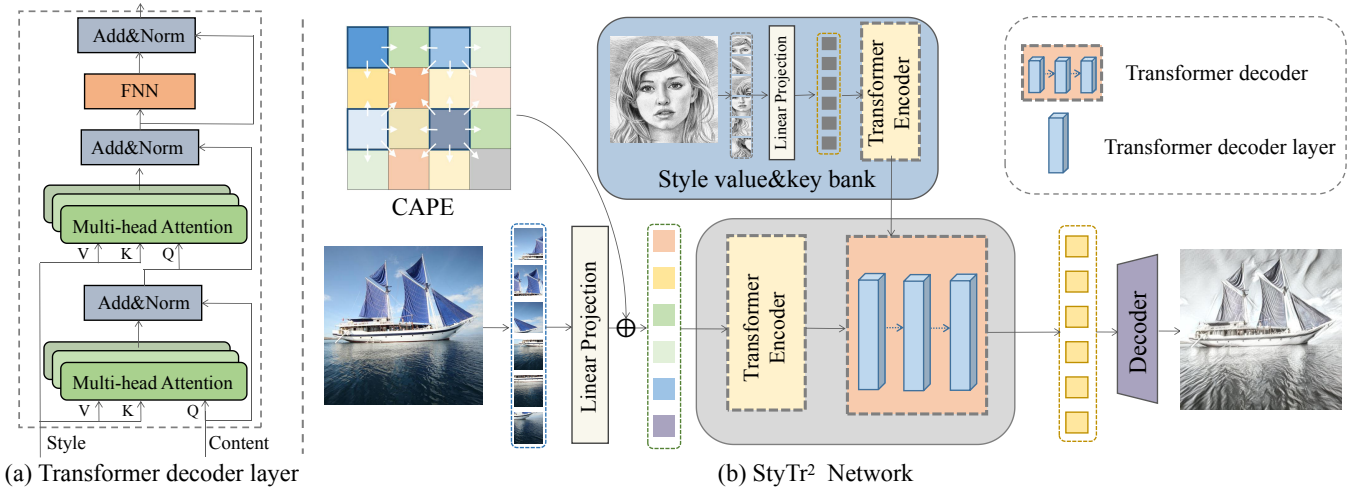


Fig. 3. The overall pipeline of our StyTr² framework. We split the content and style images into patches, and use a linear projection to obtain image sequences. Then the content sequences added with COPE are fed into the content transformer encoder, while the style sequences are fed into the style transformer encoder. Following the two transformer encoders, a multi-layer transformer decoder is adopted to stylize the content sequences according to the style sequences. Finally, we use a progressive upsampling decoder to obtain the stylized images with high-resolution.

combine multi-style in one model and achieve outstanding stylized results. More generally, arbitrary style transfer gains more attention in recent years. Huang et al. [6] propose an adaptive instance normalization (AdaIN) to replace the mean and variance of content with that of style, and achieve arbitrary style transfer. AdaIN is widely adopted in image generation tasks [10], [11], [14], [27], [28] to fuse the content and style features. Li et al. [7] design a whiten and colorization transformation (WCT) to align the second-order statistics of content and style features. Moreover, many works [20], [29], [30] aim at promoting the generation effect in the premise of efficiency. Based on the CNNs model, [15]–[17] introduce self-attention to the encoder-transfer-decoder framework for better feature fusion. However, the existing encoder-transfer-decoder style transfer methods can not handle the long-range dependencies and could lead to content leak.

b) Transformer.: Transformer [21] is first proposed for machine translation tasks, dispensing with recurrence and convolutions entirely. Based on attention mechanisms, the transformer can obtain long-range dependencies for the input sequence without considering the token ordering. Therefore, instead of recurrent neural networks [31], transformer is widely used in various NLP tasks [32]–[37]. Inspired by breakthrough of transformer in NLP, many researchers put forward vision transformers for various image tasks, including object detection [38]–[40], segmentation [41], [42], image classification [43]–[46], image processing and generation [19], [45], [47]. Traditionally CNNs are designed to learn the local correlations within images containing inductive biases. Compared with the fully convolutional network (FCN), the transformer-based networks can capture long-term dependencies of the input image by using self-attention mechanisms. In this paper, we adopt transformer structures to image style transfer tasks which can be seen as an image sequence-to-sequence generation task.

c) Positional encoding.: Positional encoding is commonly used in transformer-based models to provide position information. There are two types of positional encoding, i.e., *functional* and *parametric* positional encoding. Functional positional encoding is calculated by pre-defined functions, such as sinusoidal functions [21]. Parametric positional encoding is learned via model training [34]. To ensure translational-invariance for the transformers, relative positional encoding [48]–[51] considers the distance between tokens in the image sequence. [52], [53] further includes positional encoding in CNN-based models as spatial inductive. We propose the content-aware positional encoding that is scale-invariant and more suitable for image generation tasks.

III. METHODOLOGY

To involve the long-range dependencies of transformers into unbiased image style transfer, we formulate the image style transfer task as a sequential image generation problem. Given an input content image $I_c \in \mathbb{R}^{H \times W \times 3}$ and a style image $I_s \in \mathbb{R}^{H \times W \times 3}$, we split the images into patches (similar to tokens in the NLP tasks), and use a linear projection layer to project the input patches into a sequence feature embedding \mathcal{E} with the shape of $L \times C$, where $L = \frac{H \times W}{m \times m}$ is the length of \mathcal{E} , $m = 8$ is the patch size and C is the dimension of \mathcal{E} . The overall structure of StyTr² is shown in Figure 3.

A. Content-Aware Positional Encoding

When using a transformer-based model, the positional encoding (PE) should be included in the input sequence to acquire structure information. We analyze the impact of PE on attention calculation. According to [21], the attention score of the i -th patch and j -th patch is calculated by:

$$\begin{aligned} A_{i,j} &= ((\mathcal{E}_i + \mathcal{P}_i)W_q)^T((\mathcal{E}_j + \mathcal{P}_j)W_k) \\ &= W_q^T \mathcal{E}_i^T \mathcal{E}_j W_k + W_q^T \mathcal{E}_i^T \mathcal{P}_j W_k + W_q^T \mathcal{P}_i^T \mathcal{E}_j W_k + W_q^T \mathcal{P}_i^T \mathcal{P}_j W_k, \end{aligned} \quad (1)$$

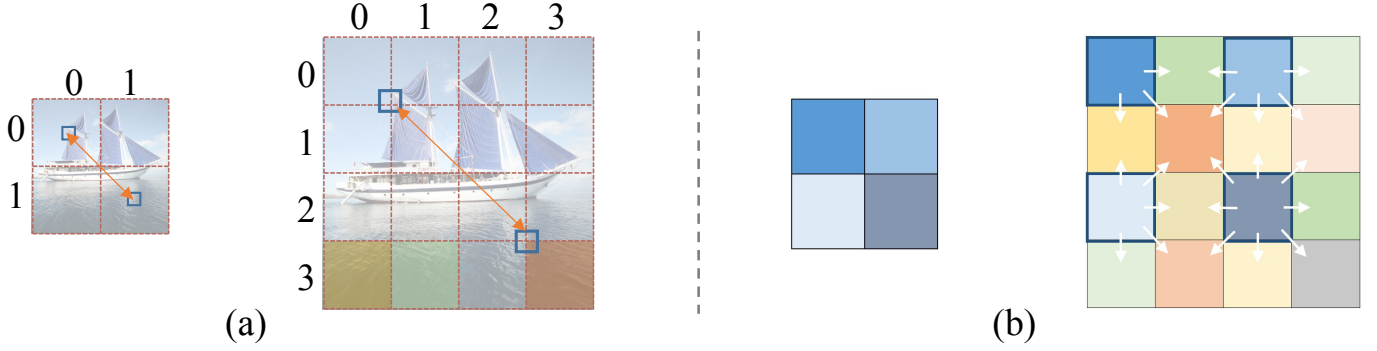


Fig. 4. Schematic diagram of content-aware positional encoding.

where W_q, W_k are parameter matrices for query and key calculation, \mathcal{P}_i presents the i -th one-dimension PE. In 2D cases, sinusoidal positional encoding is computed as:

$$\begin{aligned} \mathcal{P}_{(x_i, 2k)} &= \sin(x_i/10000^{2k/128}), \mathcal{P}_{(x_i, 2k+1)} = \cos(x_i/10000^{2k/128}), \\ \mathcal{P}_{(y_i, 2k)} &= \sin(y_i/10000^{2k/128}), \mathcal{P}_{(y_i, 2k+1)} = \cos(y_i/10000^{2k/128}). \end{aligned} \quad (2)$$

Then the positional relative relation between (x_i, y_i) patch and (x_j, y_j) patch can be written as:

$$\mathcal{P}(x_i, y_i)^T \mathcal{P}(x_j, y_j) = \sum_{k=0}^{\frac{d}{4}-1} [\cos(w_k(x_j - x_i)) + \cos(w_k(y_j - y_i))], \quad (3)$$

where $w_k = 1/10000^{2k/128}$, $d = 512$. As shown in Equation 3, the positional relative relation between two patches is merely pertinent to the distance between them. In response to this derivation result, we raise two questions: (1) for the image generation task, when calculating PE, should we take the image semantic into consideration? Traditional PE is designed for sentences ordered by logic, but the image patch sequences are organized by image content. We express the distance between two patches as $d(\cdot)$. In the right side of Figure 4(a), the difference between $d((x_3, y_0), (x_3, y_1))$ and $d((x_3, y_0), (x_3, y_3))$ should be small, because we expect the similar content patches have similar stylized results; (2) is the traditional sinusoidal positional encoding still suitable for vision tasks when the input image size expands exponentially? In Figure 4(a), when resizing the input images, the relative relation between patches (blue blocks) in the same semantic can change dramatically, which may be not suitable for multi-size input in vision tasks.

Therefore, we propose content-aware positional encoding (CAPE) which is scale-invariant and more suitable for style transfer task. Different from sinusoidal PE that only considers the relative distance of patches, CAPE is conditioned on the image content semantic. We assume that $n \times n$ is adequate for expressing the semantic positions for every image. For an image $I \in \mathbb{R}^{H \times W \times 3}$, we rescale the fixed $n \times n$ positional encoding to $\frac{H}{n} \times \frac{W}{n}$ as shown in Figure 4(b). In this way, various image scales will not influence the position relation between two image patches. The CAPE of patch (x, y) is formulated as $\mathcal{P}_{CA}(x, y)$ following:

$$\mathcal{P}_L = \mathcal{F}_{pos}(\text{AveragePool}_{n \times n}(\mathcal{E})), \quad \mathcal{P}_{CA}(x, y) = \sum_{i=0}^s \sum_{j=0}^s (a_{ij} \mathcal{P}_L(x_i, y_j)), \quad (4)$$

\mathcal{F}_{pos} is a learnable positional encoding function, \mathcal{P}_L is learnable PE following the sequence \mathcal{E} , n is set to 18 through experiments, a_{ij} is the interpolation weight, s is the number of neighbors. Finally, for i -th patch $\mathcal{E}_i \in \mathbb{R}^C$ at position (x, y) in sequence \mathcal{E} , we add \mathcal{P}_{CA_i} to \mathcal{E}_i to form the final sequence.

B. Style Transfer Transformer

a) *Transformer encoder.*: We gain long-range dependencies of image sequences by using transformer structure to learn sequential representation for input images. Different from most vision tasks [38], [40], [47], the inputs of the style transfer task belong to two very different domains, usually including artistic paintings and natural images. Therefore, *StyleTr²* has two transformer encoders to encode domain-specific features, which are used to translate a sequence from one domain to another domain in the next stage.

Given an content sequence $Z_c = \{\mathcal{E}_{c1} + \mathcal{P}_{CA1}, \mathcal{E}_{c2} + \mathcal{P}_{CA2}, \dots, \mathcal{E}_{cL} + \mathcal{P}_{CAL}\}$, we first feed it to the transformer encoder layers. Every transformer encoder layer consists of a multi-head self-attention module (MSA) and a feed-forward network (FFN). The input sequence is encoded into query (Q), key (K) and value (V):

$$Q = Z_c W_q, \quad K = Z_c W_k, \quad V = Z_c W_v, \quad (5)$$

where $W_q, W_k, W_v \in \mathbb{R}^{C \times d_{head}}$. The multi-head attention is then calculated by:

$$\mathcal{F}_{MSA}(Q, K, V) = \text{Concat}(\text{Attention}_1(Q, K, V), \dots, \text{Attention}_N(Q, K, V))W_o, \quad (6)$$

where $W_o \in \mathbb{R}^{C \times C}$ are learnable parameters, N is the number of attention heads, and $d_{head} = \frac{C}{N}$. The residual connections are applied to obtain the output content sequence:

$$\begin{aligned} Y'_c &= \mathcal{F}_{MSA}(Q, K, V) + Q, \\ Y_c &= \mathcal{F}_{FFN}(Y'_c) + Y'_c, \end{aligned} \quad (7)$$

where $\mathcal{F}_{FFN}(Y'_c) = \max(0, Y'_c W_1 + b_1) W_2 + b_2$. In addition, layernorm (LN) is applied after every block [21].

The style sequence $Z_s = \{\mathcal{E}_{s1}, \mathcal{E}_{s2}, \dots, \mathcal{E}_{sL}\}$ is encoded into sequence Y_s following the same calculation process except for not considering the style positional encoding, since we do not need to maintain the style structures in the final output.

b) Transformer decoder: The transformer decoder layers are used to translate the content sequence according to the referenced style sequence in a regressive fashion. Different from the auto-regressive process in NLPs, we use all sequence patches as inputs at one time to predict the output. As shown in Figure 4(a), every transformer decoder layer contains two MSA layers and one FFN. The inputs of transformer decoder are the content sequence with CAPE $\hat{Y}_c = \{Y_{c1} + \mathcal{P}_{CA1}, Y_{c2} + \mathcal{P}_{CA2}, \dots, Y_{cL} + \mathcal{P}_{CAL}\}$ and style sequence $Y_s = \{Y_{s1}, Y_{s2}, \dots, Y_{sL}\}$. We use the content sequence to generate Q , and use style sequence to generate K and V .

$$Q = \hat{Y}_c W_q, \quad K = Y_s W_k, \quad V = Y_s W_v. \quad (8)$$

Then, the output of the transformer decoder can be calculated by:

$$\begin{aligned} X'' &= \mathcal{F}_{MSA}(Q, K, V) + Q, \\ X' &= \mathcal{F}_{MSA}(X'' + \mathcal{P}_{CA}, K, V) + X'', \\ X &= \mathcal{F}_{FFN}(X') + X'. \end{aligned} \quad (9)$$

Layernorm (LN) is also applied after every block [21].

c) Decoder: The output sequence of the transformer is in the shape of $\frac{HW}{64} \times C$. Instead of directly upsampling the outputs for constructing the results, we employ a three-layer CNN decoder to refine the outputs of transformer decoder following [41]. For each layer, we expand the scale by adopting a $3 \times 3 \text{ Conv} + \text{ReLU} + 2 \times \text{upsampling}$ operation. Finally, we can obtain the output results in $H \times W \times 3$.

C. Optimization

The generated optimal results should maintain the original content structures while transferred vivid referenced style patterns. As described in [3], the feature maps extracted by VGG can be used as content features to represent image structures. The Gram matrix of feature maps can be used as style features to represent color, texture. Therefore, we construct perceptual content loss to measure the content differences between generated images I_{cs} and I_c , perceptual style loss to measure the style differences between I_{cs} and I_c .

The content perceptual loss is defined as:

$$\mathcal{L}_c = \frac{1}{N_l} \sum_{i=0}^{N_l} \|\phi_i(I_{cs}) - \phi_i(I_c)\|_2. \quad (10)$$

$\phi_i(\cdot)$ denotes the features extracted from the i -th layer in a pretrained VGG19. The statistics (e.g., mean and variance) of neural network layers contains traits of different domains [7]. Therefore, we use the style perceptual loss defined as:

$$\mathcal{L}_s = \frac{1}{N_l} \sum_{i=0}^{N_l} \|\mu(\phi_i(I_{cs})) - \mu(\phi_i(I_s))\|_2 + \|\sigma(\phi_i(I_{cs})) - \sigma(\phi_i(I_s))\|_2. \quad (11)$$

$\mu(\cdot)$ denotes the mean of features, and $\sigma(\cdot)$ denotes the variance of features. Self-supervised learning [54] uses a pretext to mine its supervision information from large-scale unsupervised data. The network can be trained with such constructed supervision information to learn valuable representations for downstream tasks. Therefore, we adopt an auxiliary self-style transfer task to learn the richer and more accurate semantic and style representation. We input two same content (style) images into our *StyTr*², the generated image $I_{cc}(I_{ss})$ should be identical to the $I_c(I_s)$. Therefore, the identity loss simulates the differences between $I_c(I_s)$ and $I_{cc}(I_{ss})$:

$$\begin{aligned} \mathcal{L}_{id1} &= \|I_{cc} - I_c\|_2 + \|I_{ss} - I_s\|_2, \\ \mathcal{L}_{id2} &= \frac{1}{N_l} \sum_{i=0}^{N_l} \|\phi_i(I_{cc}) - \phi_i(I_c)\|_2 + \|\phi_i(I_{ss}) - \phi_i(I_s)\|_2. \end{aligned} \quad (12)$$

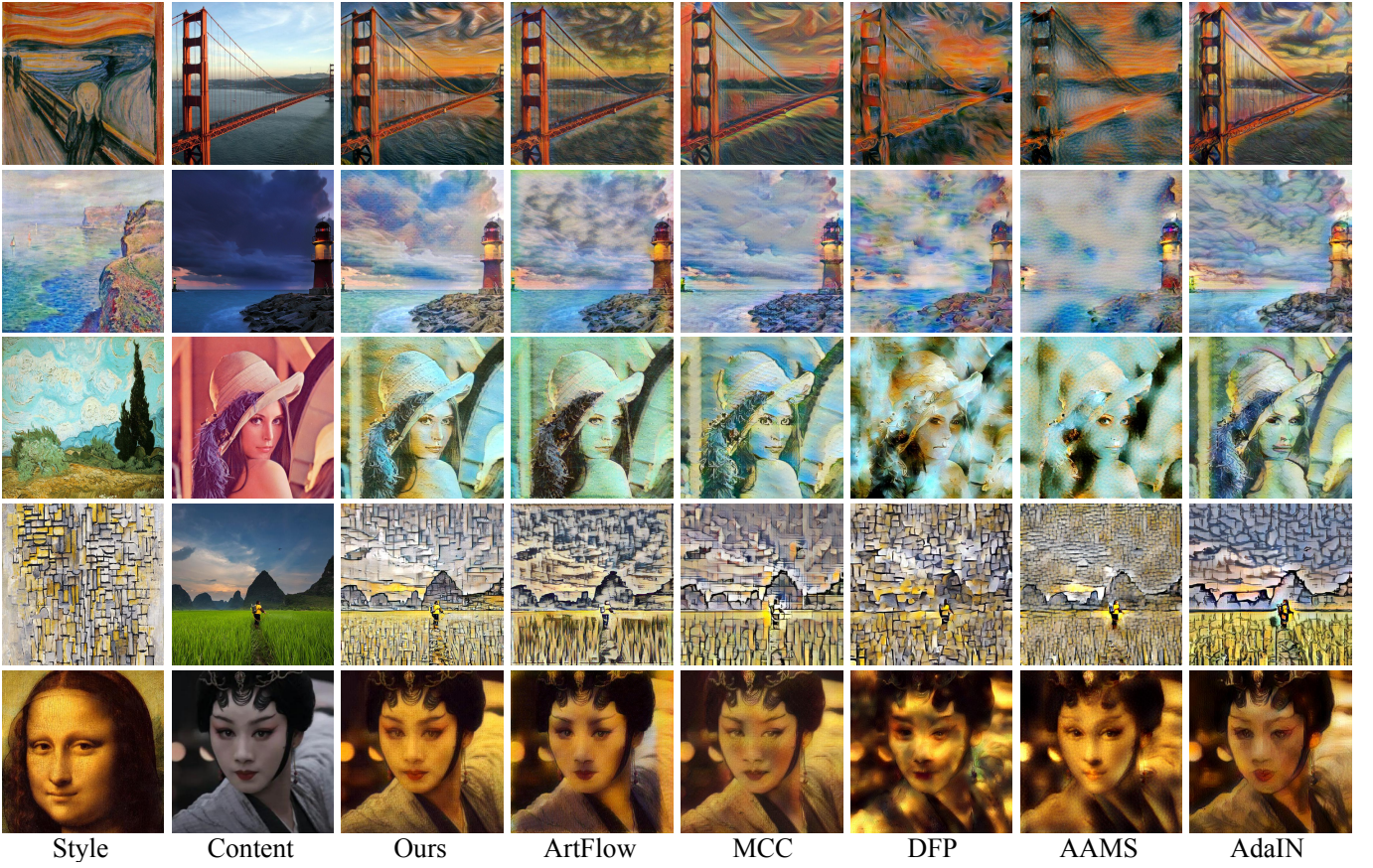


Fig. 5. Comparisons of style transfer results using different methods.

The whole network is optimized by minimizing the following function:

$$\mathcal{L} = \lambda_c \mathcal{L}_c + \lambda_s \mathcal{L}_s + \lambda_{id1} \mathcal{L}_{id1} + \lambda_{id2} \mathcal{L}_{id2}. \quad (13)$$

We set λ_c , λ_s , λ_{id1} , and λ_{id2} to 10, 7, 50, and 1 to eliminate the impact of magnitude differences.

IV. EXPERIMENTS

A. Implementation Details

MS-COCO [55] is used as the content dataset and WikiArt [56] is used as the style dataset. In the training stage, all images are randomly cropped into 256×256 , while in the testing stage, any image size is supported. We adopt the Adam [57] optimizer and the learning rate is set to 0.0005 using the warm-up adjustment strategy [58].

B. Comparisons with SOTAs

We compare our method with AdaIN [6], AAMS [18], DFP [8], MCC [17] and ArtFlow [20]. AdaIN [6] uses adaptive instance normalization to assign the mean and variance of the style images to the content images to achieve universal style transfer. AAMS [18] consists of a self-attention autoencoder capturing the main structures of the content images, and a multi-stroke style transfer model based on patch-swap [59]. DFP [8] is based on WCT [7] and uses an orthogonal random noise matrix to generate diversified stylized results. MCC [17] is a video style transfer method but can be applied to images without damaging the generated results. ArtFlow [20] designs a projection flow network (PFN) to replace the CNN-based structure to avoid the image reconstruction error and image recovery bias. Transfer modules in AdaIN and WCT can be flexibly adopted in the PFN-based model to achieve an unbiased style transfer. In our experiments, we use the AdaIN + ArtFlow version.

a) *Qualitative evaluation.*: The visual results are shown in Figure 5. Due to the simplified alignment of mean and variance, the results generated by AdaIN have insufficient style patterns. The stylized images have the crack effect which affects the overall transfer performance. Moreover, the color distribution is quite strange in some stylized images (the 2nd and 4th rows). AAMS focuses on the main structures in the content image, but ignore the non-main structures. Therefore, the secondary structures are buried. Besides, the patch-swap-based method leads to obvious patch stitching traces. Although DFP can generate results with vivid style patterns, the content structures are highly damaged. MCC uses a transform formulation of self-attention, but the absence of non-linear operation leads to object edge overflow effect (the 1st and 3rd rows). The PFN-based model

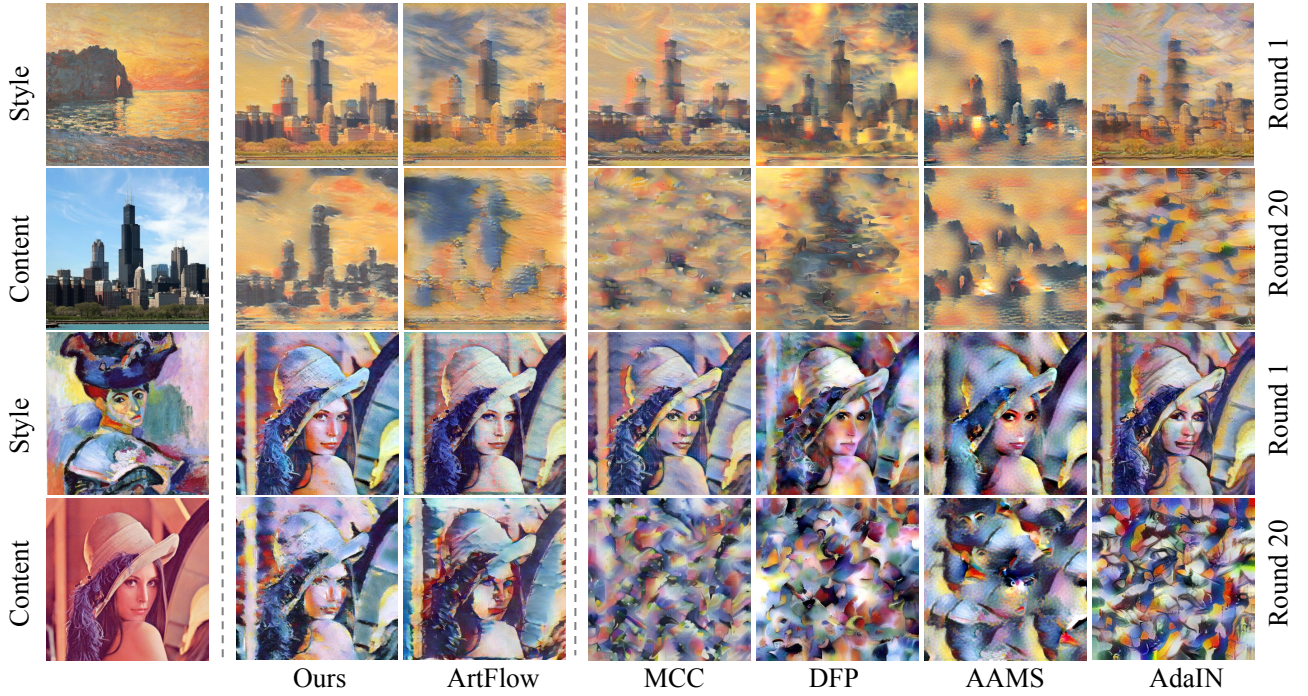


Fig. 6. Comparisons of the biased and unbiased methods.

\downarrow	Ours	ArtFlow	MCC	DFP	AAMS	AdaIN
\mathcal{L}_c	1.91	2.13	2.38	2.67	2.44	2.34
\mathcal{L}_s	1.47	3.08	1.56	2.12	3.18	1.91

TABLE I
QUANTITATIVE COMPARISONS.

	ArtFlow	MCC	DFP	AAMS	AdaIN
rates of votes	25.7	25.5	22.6	18.2	23.5

TABLE II
USER STUDY RESULTS.

has weak feature representation ability, thus ArtFlow faces the problem of style pattern deficiency. The border of stylized images has the problem of numerical overflow. By contrast, StyTr² uses the transformer structure which has a stronger feature representation ability to generate stylized results. Therefore, the results generated by StyTr² can maintain the refined content structures and abundant style patterns.

b) Unbiased style transfer.: As described in Section I, the inductive biases in CNN-based style transfer structures will lead to the content leak. The content leak is easy to spot by eyes through several rounds of stylization process [20]. We show the 1st round and 20th rounds stylization results in Figure 6. With the increase of the stylization rounds, the content structures generated by the CNN-based methods (MCC, DFP, AAMA, and AdaIN) blur out, while the content structures generated by us are still distinct. Compared with ArtFlow which is designed to solve the content leak problem of the CNN-based style transfer method, we can also conclude that our method has a strong ability to avoid content leak. Moreover, our model has better feature representation ability (the style patterns in the results generated by ArtFlow are inferior).

c) Quantitative evaluation.: We randomly select 40 style images and 20 content images to generate 800 stylized images. For each method, we calculate the content differences between stylized images and content images defined in Equation 10, and calculate the style differences between stylized images and style images defined in Equation 11. Table I presents quantitative results. Our method can achieve both low content and style loss, and make a perfect balance between content and style.



Fig. 7. Comparisons of sinusoidal PE and CAPE using content images with repetitive patterns.



Fig. 8. Comparisons of sinusoidal PE and CAPE using content images with variational resolutions.

d) User study.: To further compare our method with state-of-the-art methods, we conduct a user study to measure how much the public like the results of the different methods. We use the images in quantitative comparison and invite 100 participants to be involved in our user study. For each participant, we show him/her 40 choice questions. The question is that, given a content image and a style image, we show the result generated by our method and the result generated by a random comparison method, and we want the user to choose which result has better stylization effects. Finally, we count the votes and show the statistical results in Table II. We can conclude that our method wins by a landslide compared with any other method.

C. Analysis of CAPE

As described in Section 3.1, when calculating PE, we should take the image semantic into account. To compare the proposed CAPE with sinusoidal PE which is semantic-free, we show two cases where the input content image has repetitive patterns or is simply collaged by repeating one image four times. As shown in Figure 7, we can observe obviously discrepant stylized regions in the stylized results when using sinusoidal PE. Note that the input image size is set to 256×256 , which is the same as the resolution of the image during training, to avoid the scale variation.

Moreover, vision tasks face the problem of different input resolutions. The drastic increase of image resolution leads to huge changes in traditional PE. An ideal PE for vision tasks should be scale-invariant. For the sake of an intuitive comparison, we also use the sinusoidal PE to replace our CAPE. Figure 8 shows some contrast results. In the third row of Figure 8, the input image size is 512×512 , which is the double of the image resolution during training. Not surprisingly, the generated results appear vertical track defects due to the huge position deviation. In the second row of Figure 8, the input image size is 256×256 , which is the same as the image resolution during training. The vertical track defect is disappeared, but the results are not that satisfactory due to the small resolution. By contrast, our method supports any input size with CAPE. Meanwhile, our results in the last row of Figure 8 present both clear content structures and proper stylized patterns. More ablation studies can be seen in the supplementary materials.

V. CONCLUSION

In this work, we propose StyTr² for unbiased image style transfer. Our StyTr² includes a content transformer encoder and a style transformer encoder for extraction of domain-specific long-range information. A progressive transformer decoder is remoulded to translate the content sequences based on the referenced style sequences. We also propose the content-aware positional encoding which is suitable for vision generation tasks. The content-aware positional encoding is conditioned on image semantics and can be expanded to any size without positional deviation. In general, our StyTr² is the first transformer-based style transfer method, which get rid of the content leak problem of CNN-based models and can be used to generate outstanding stylized results.

REFERENCES

- [1] A. A. Efros and W. T. Freeman, "Image quilting for texture synthesis and transfer," in *Proceedings of Annual Conference on Computer Graphics and Interactive Techniques*, 2001, pp. 341–346.
- [2] S. Bruckner and M. E. Gröller, "Style transfer functions for illustrative volume rendering," *Computer Graphics Forum*, vol. 26, no. 3, pp. 715–724, 2007.

- [3] L. A. Gatys, A. S. Ecker, and M. Bethge, “Image style transfer using convolutional neural networks,” in *IEEE/CVF Conference on Computer Vision and Pattern Recognition (CVPR)*. IEEE, 2016, pp. 2414–2423.
- [4] Y. Li, N. Wang, J. Liu, and X. Hou, “Demystifying neural style transfer,” in *International Joint Conference on Artificial Intelligence (IJCAI)*, 2017.
- [5] E. Risser, P. Wilmot, and C. Barnes, “Stable and controllable neural texture synthesis and style transfer using histogram losses,” *arXiv preprint arXiv:1701.08893*, 2017.
- [6] X. Huang and B. Serge, “Arbitrary style transfer in real-time with adaptive instance normalization,” in *IEEE International Conference on Computer Vision (ICCV)*. IEEE, 2017, pp. 1501–1510.
- [7] Y. Li, C. Fang, J. Yang, Z. Wang, X. Lu, and M.-H. Yang, “Universal style transfer via feature transforms,” in *Advances Neural Information Processing Systems (NeurIPS)*, 2017, pp. 386–396.
- [8] Z. Wang, L. Zhao, H. Chen, L. Qiu, Q. Mo, S. Lin, W. Xing, and D. Lu, “Diversified arbitrary style transfer via deep feature perturbation,” in *IEEE/CVF Conference on Computer Vision and Pattern Recognition (CVPR)*, 2020, pp. 7789–7798.
- [9] Y. Li, M.-Y. Liu, X. Li, M.-H. Yang, and J. Kautz, “A closed-form solution to photorealistic image stylization,” in *European Conference on Computer Vision (ECCV)*, 2018, pp. 453–468.
- [10] T. Lin, Z. Ma, F. Li, D. He, X. Li, E. Ding, N. Wang, J. Li, and X. Gao, “Drafting and revision: Laplacian pyramid network for fast high-quality artistic style transfer,” in *IEEE/CVF Conference on Computer Vision and Pattern Recognition (CVPR)*, 2021.
- [11] J. An, T. Li, H. Huang, L. Shen, X. Wang, Y. Tang, J. Ma, W. Liu, and J. Luo, “Real-time universal style transfer on high-resolution images via zero-channel pruning,” *arXiv preprint arXiv:2006.09029*, 2020.
- [12] M. Lu, H. Zhao, A. Yao, Y. Chen, F. Xu, and L. Zhang, “A closed-form solution to universal style transfer,” *IEEE/CVF International Conference on Computer Vision (ICCV)*, 2019.
- [13] J. An, H. Xiong, J. Huan, and J. Luo, “Ultrafast photorealistic style transfer via neural architecture search,” in *AAAI Conference on Artificial Intelligence (AAAI)*, vol. 34, 2020, pp. 10443–10450.
- [14] H. Wang, Y. Li, Y. Wang, H. Hu, and M.-H. Yang, “Collaborative distillation for ultra-resolution universal style transfer,” in *IEEE/CVF Conference on Computer Vision and Pattern Recognition*, 2020, pp. 1860–1869.
- [15] D. Y. Park and K. H. Lee, “Arbitrary style transfer with style-attentional networks,” in *IEEE/CVF Conference on Computer Vision and Pattern Recognition (CVPR)*. IEEE, 2019, pp. 5880–5888.
- [16] Y. Deng, F. Tang, W. Dong, W. Sun, F. Huang, and C. Xu, “Arbitrary style transfer via multi-adaptation network,” in *ACM International Conference on Multimedia*, 2020, pp. 2719–2727.
- [17] Y. Deng, F. Tang, W. Dong, H. Huang, C. Ma, and C. Xu, “Arbitrary video style transfer via multi-channel correlation,” in *AAAI Conference on Artificial Intelligence (AAAI)*, 2021.
- [18] Y. Yao, J. Ren, X. Xie, W. Liu, Y.-J. Liu, and J. Wang, “Attention-aware multi-stroke style transfer,” in *IEEE/CVF Conference on Computer Vision and Pattern Recognition (CVPR)*. IEEE, 2019, pp. 1467–1475.
- [19] Y. Jiang, S. Chang, and Z. Wang, “Transgan: Two transformers can make one strong gan,” *arXiv preprint arXiv:2102.07074*, 2021.
- [20] J. An, S. Huang, Y. Song, D. Dou, W. Liu, and J. Luo, “ArtFlow: Unbiased image style transfer via reversible neural flows,” in *IEEE/CVF Conferences on Computer Vision and Pattern Recognition (CVPR)*, 2021.
- [21] A. Vaswani, N. Shazeer, N. Parmar, J. Uszkoreit, L. Jones, A. N. Gomez, L. Kaiser, and I. Polosukhin, “Attention is all you need,” in *Advances in Neural Information Processing Systems (NeurIPS)*, 2017.
- [22] P. W. Battaglia, J. B. Hamrick, V. Bapst, A. Sanchez-Gonzalez, V. Zambaldi, M. Malinowski, A. Tacchetti, D. Raposo, A. Santoro, R. Faulkner *et al.*, “Relational inductive biases, deep learning, and graph networks,” *arXiv preprint arXiv:1806.01261*, 2018.
- [23] J. Johnson, A. Alahi, and L. Fei-Fei, “Perceptual losses for real-time style transfer and super-resolution,” in *European Conference on Computer Vision (ECCV)*. Springer, 2016, pp. 694–711.
- [24] C. Li and M. Wand, “Precomputed real-time texture synthesis with markovian generative adversarial networks,” in *European Conference on Computer Vision (ECCV)*, 2016, pp. 702–716.
- [25] D. Chen, L. Yuan, J. Liao, N. Yu, and G. Hua, “Stylebank: An explicit representation for neural image style transfer,” in *IEEE/CVF Conference on Computer Vision and Pattern Recognition (CVPR)*, 2017, pp. 1897–1906.
- [26] V. Dumoulin, J. Shlens, and M. Kudlur, “A learned representation for artistic style,” in *International Conference on Learning Representations (ICLR)*, 2016.
- [27] T. Karras, S. Laine, and T. Aila, “A style-based generator architecture for generative adversarial networks,” in *IEEE/CVF Conference on Computer Vision and Pattern Recognition (CVPR)*, 2019, pp. 4401–4410.
- [28] X. Huang, M.-Y. Liu, S. Belongie, and J. Kautz, “Multimodal unsupervised image-to-image translation,” in *European conference on computer vision (ECCV)*, 2018, pp. 172–189.
- [29] Z. Wu, C. Song, Y. Zhou, M. Gong, and H. Huang, “Efanet: Exchangeable feature alignment network for arbitrary style transfer,” in *AAAI Conference on Artificial Intelligence (AAAI)*, 2020, pp. 12305–12312.
- [30] J. Svoboda, A. Anoosheh, C. Osendorfer, and J. Masci, “Two-stage peer-regularized feature recombination for arbitrary image style transfer,” in *IEEE/CVF Conference on Computer Vision and Pattern Recognition (CVPR)*, 2020, pp. 13816–13825.
- [31] J. Chung, C. Gulcehre, K. Cho, and Y. Bengio, “Empirical evaluation of gated recurrent neural networks on sequence modeling,” in *Advances in Neural Information Processing Systems (NeurIPS)*, 2014.
- [32] A. Radford, J. Wu, R. Child, D. Luan, D. Amodei, and I. Sutskever, “Language models are unsupervised multitask learners,” *OpenAI blog*, vol. 1, no. 8, p. 9, 2019.
- [33] T. B. Brown, B. Mann, N. Ryder, M. Subbiah, J. Kaplan, P. Dhariwal, A. Neelakantan, P. Shyam, G. Sastry, A. Askell *et al.*, “Language models are few-shot learners,” in *Advances in Neural Information Processing Systems (NeurIPS)*, 2020, pp. 1877–1901.
- [34] J. Devlin, M.-W. Chang, K. Lee, and K. Toutanova, “Bert: Pre-training of deep bidirectional transformers for language understanding,” in *Conference of the North American Chapter of the Association for Computational Linguistics: Human Language Technologies, Volume 1 (Long and Short Papers)*, 2019, pp. 4171–4186.
- [35] Y. Liu, M. Ott, N. Goyal, J. Du, M. Joshi, D. Chen, O. Levy, M. Lewis, L. Zettlemoyer, and V. Stoyanov, “Roberta: A robustly optimized bert pretraining approach,” *arXiv preprint arXiv:1907.11692*, 2019.
- [36] A. Radford, K. Narasimhan, T. Salimans, and I. Sutskever, “Improving language understanding by generative pre-training,” *Preprint*, 2018.
- [37] N. Dai, J. Liang, X. Qiu, and X. Huang, “Style transformer: Unpaired text style transfer without disentangled latent representation,” in *Annual Meeting of the Association for Computational Linguistics (ACL)*, 2019.
- [38] N. Carion, F. Massa, G. Synnaeve, N. Usunier, A. Kirillov, and S. Zagoruyko, “End-to-end object detection with transformers,” in *European Conference on Computer Vision (ECCV)*, 2020, pp. 213–229.
- [39] X. Zhu, W. Su, L. Lu, B. Li, X. Wang, and J. Dai, “Deformable detr: Deformable transformers for end-to-end object detection,” in *International Conference on Learning Representations (ICLR)*, 2021.
- [40] Z. Dai, B. Cai, Y. Lin, and J. Chen, “Up-detr: Unsupervised pre-training for object detection with transformers,” in *IEEE/CVF Conference on Computer Vision and Pattern Recognition (CVPR)*, 2021.
- [41] S. Zheng, J. Lu, H. Zhao, X. Zhu, Z. Luo, Y. Wang, Y. Fu, J. Feng, T. Xiang, P. H. Torr, and L. Zhang, “Rethinking semantic segmentation from a sequence-to-sequence perspective with transformers,” in *IEEE/CVF Conference on Computer Vision and Pattern Recognition (CVPR)*, 2021.

- [42] Y. Wang, Z. Xu, X. Wang, C. Shen, B. Cheng, H. Shen, and H. Xia, "End-to-end video instance segmentation with transformers," in *IEEE/CVF Conference on Computer Vision and Pattern Recognition(CVPR)*, 2021.
- [43] A. Dosovitskiy, L. Beyer, A. Kolesnikov, D. Weissenborn, X. Zhai, T. Unterthiner, M. Dehghani, M. Minderer, G. Heigold, S. Gelly *et al.*, "An image is worth 16x16 words: Transformers for image recognition at scale," in *International Conference on Learning Representations (ICLR)*, 2021.
- [44] B. Wu, C. Xu, X. Dai, A. Wan, P. Zhang, M. Tomizuka, K. Keutzer, and P. Vajda, "Visual transformers: Token-based image representation and processing for computer vision," *arXiv preprint arXiv:2006.03677*, 2020.
- [45] M. Chen, A. Radford, R. Child, J. Wu, H. Jun, D. Luan, and I. Sutskever, "Generative pretraining from pixels," in *International Conference on Machine Learning(ICML)*, 2020, pp. 1691–1703.
- [46] Z. Liu, Y. Lin, Y. Cao, H. Hu, Y. Wei, Z. Zhang, S. Lin, and B. Guo, "Swin transformer: Hierarchical vision transformer using shifted windows," in *IEEE/CVF Conference on Computer Vision and Pattern Recognition (CVPR)*, 2021.
- [47] H. Chen, Y. Wang, T. Guo, C. Xu, Y. Deng, Z. Liu, S. Ma, C. Xu, C. Xu, and W. Gao, "Pre-trained image processing transformer," in *IEEE/CVF Conference on Computer Vision and Pattern Recognition (CVPR)*, 2021.
- [48] P. Shaw, J. Uszkoreit, and A. Vaswani, "Self-attention with relative position representations," in *Annual Conference of the North American Chapter of the Association for Computational Linguistics(NAAACL)*, 2018.
- [49] Z. Yang, Z. Dai, Y. Yang, J. Carbonell, R. Salakhutdinov, and Q. V. Le, "Xlnet: Generalized autoregressive pretraining for language understanding," in *Advances in Neural Information Processing Systems(NeurIPS)*, 2019.
- [50] C. Raffel, N. Shazeer, A. Roberts, K. Lee, S. Narang, M. Matena, Y. Zhou, W. Li, and P. J. Liu, "Exploring the limits of transfer learning with a unified text-to-text transformer," *Journal of Machine Learning Research*, vol. 21, no. 140, pp. 1–67, 2020.
- [51] P. He, X. Liu, J. Gao, and W. Chen, "Deberta: Decoding-enhanced bert with disentangled attention," in *International Conference on Learning Representations (ICLR)*, 2021.
- [52] R. Xu, X. Wang, K. Chen, B. Zhou, and C. C. Loy, "Positional encoding as spatial inductive bias in gans," in *IEEE/CVF Conference on Computer Vision and Pattern Recognition(CVPR)*, 2021.
- [53] M. A. Islam, S. Jia, and N. D. B. Bruce, "How much position information do convolutional neural networks encode?" in *International Conference on Learning Representations (ICLR)*, 2020.
- [54] L. Jing and Y. Tian, "Self-supervised visual feature learning with deep neural networks: A survey," *IEEE Transactions on Pattern Analysis and Machine Intelligence*, 2020.
- [55] T.-Y. Lin, M. Maire, S. Belongie, J. Hays, P. Perona, D. Ramanan, P. Dollár, and C. L. Zitnick, "Microsoft COCO: Common objects in context," in *European Conference on Computer Vision (ECCV)*, 2014, pp. 740–755.
- [56] F. Phillips and B. Mackintosh, "Wiki art gallery, inc.: A case for critical thinking," *Issues in Accounting Education*, vol. 26, no. 3, pp. 593–608, 2011.
- [57] D. P. Kingma and J. Ba, "Adam: A method for stochastic optimization," *arXiv preprint arXiv:1412.6980*, 2014.
- [58] R. Xiong, Y. Yang, D. He, K. Zheng, S. Zheng, C. Xing, H. Zhang, Y. Lan, L. Wang, and T. Liu, "On layer normalization in the transformer architecture," in *International Conference on Machine Learning(ICML)*, 2020, pp. 10 524–10 533.
- [59] T. Q. Chen and M. Schmidt, "Fast patch-based style transfer of arbitrary style," *arXiv preprint arXiv:1612.04337*, 2016.

APPENDIX

A. Network Architecture

In this section, we show the detailed sketch diagram of decoder and self-supervised learning task. (a) The decoder uses three layers of 3×3 Conv + ReLU + $2 \times$ upsample to increase the output resolution. (b) Self-supervised learning task uses the information of the input image. As shown in Figure 9, we input two same content (style) images into our $StyTr^2$, the generated image should be identical to the input content (style) image.

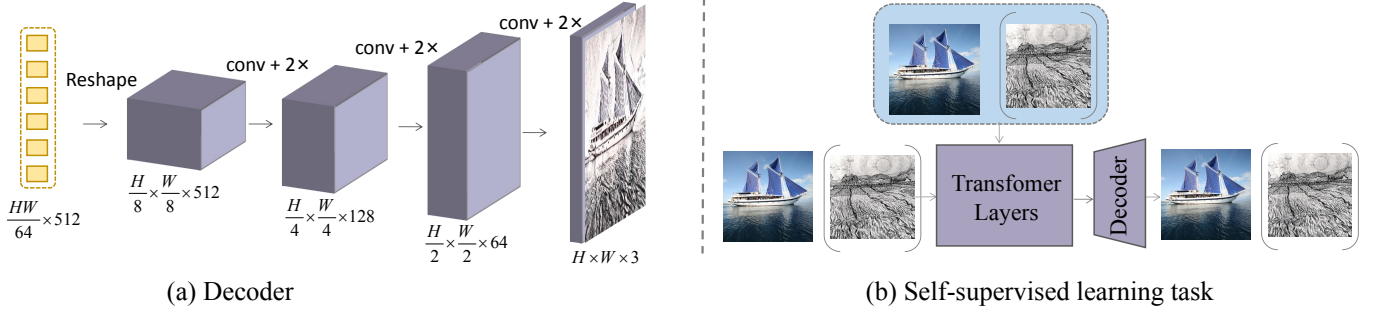


Fig. 9. Network architecture. (a) The three layers CNN-based decoder used to increase image resolution. (2) Self-supervised learning task used as a training aid.

B. Limitations

When we input a large content image of face and an abstract style image, the generated results can be rendered with plenty of style patterns (e.g., sharp edges in Figure 10) which may not be visually pleasant. The reason for the above phenomenon is that we do not consider whether the input style is suitable for the content image. In the future, we plan to take the semantic information of content and style into consideration to generate better stylization results.

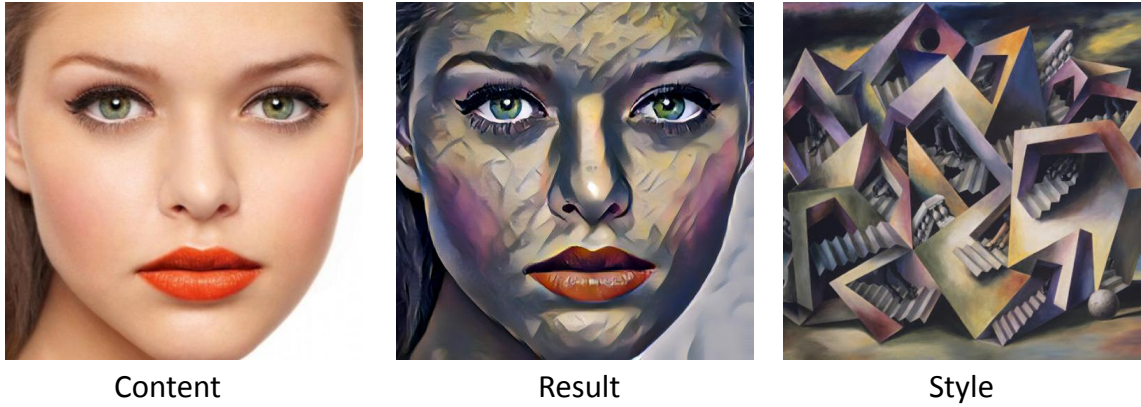


Fig. 10. Limitation of our $StyTr^2$ framework.

C. Progressive Generation

Thanks to the ability to capture long-range dependencies, transformer can be used to generate image in a progressive fashion without content leak. We use three layers transformer encoder-decoder to simulate the process of art creation from coarse to fine. As depicted in Figure 11, when removing the progressive layers and only leaving a single transformer layer, the results lose more structure details (the people in the middle), and the rendered style patterns are not that similar to the referenced style image (the square strokes in the sky). We also calculate the content loss and style loss in Table III, without the progressive calculation, the content maintaining and style transferring abilities are both degraded.

D. Image to Sequence

As described in Section 1 of the main body, the CNN-based style transfer structures introduce content leak after several rounds of the stylization process due to the inductive biases caused by locality and spatial invariance. To show the impact of CNN structures, we replace the Linear projection layer with a deep CNN projection layer to split the image into a sequence.

	Ours	Single-layer
Content loss	1.91	1.94
Style loss	1.47	2.38

TABLE III
QUANTITY COMPARISON OF PROGRESSIVE GENERATION.

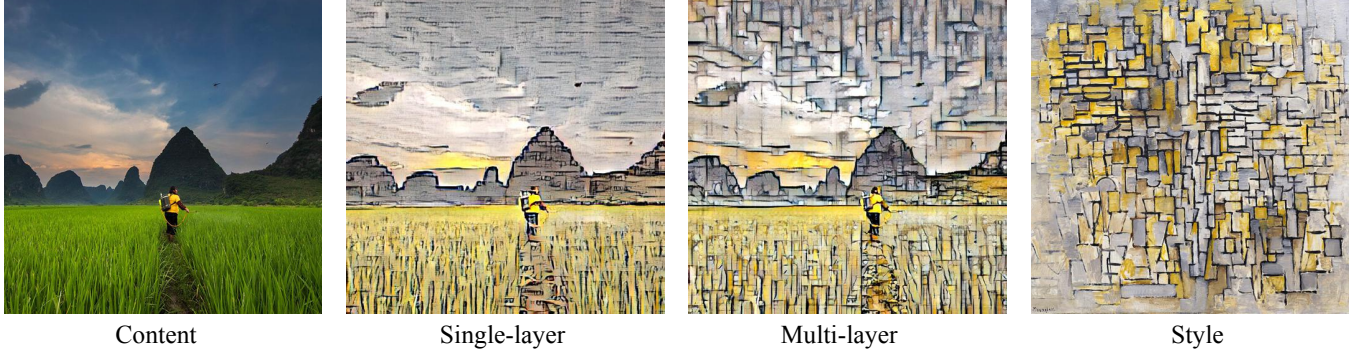


Fig. 11. The influence of progressive generation of transformer decoder.

Figure 12 shows the multiple rounds of image stylization results using different projection methods. With the increase of the stylization rounds, the content structures generated by the CNN projection layer blur out, while the content structures generated by the linear projection layer are still distinct.

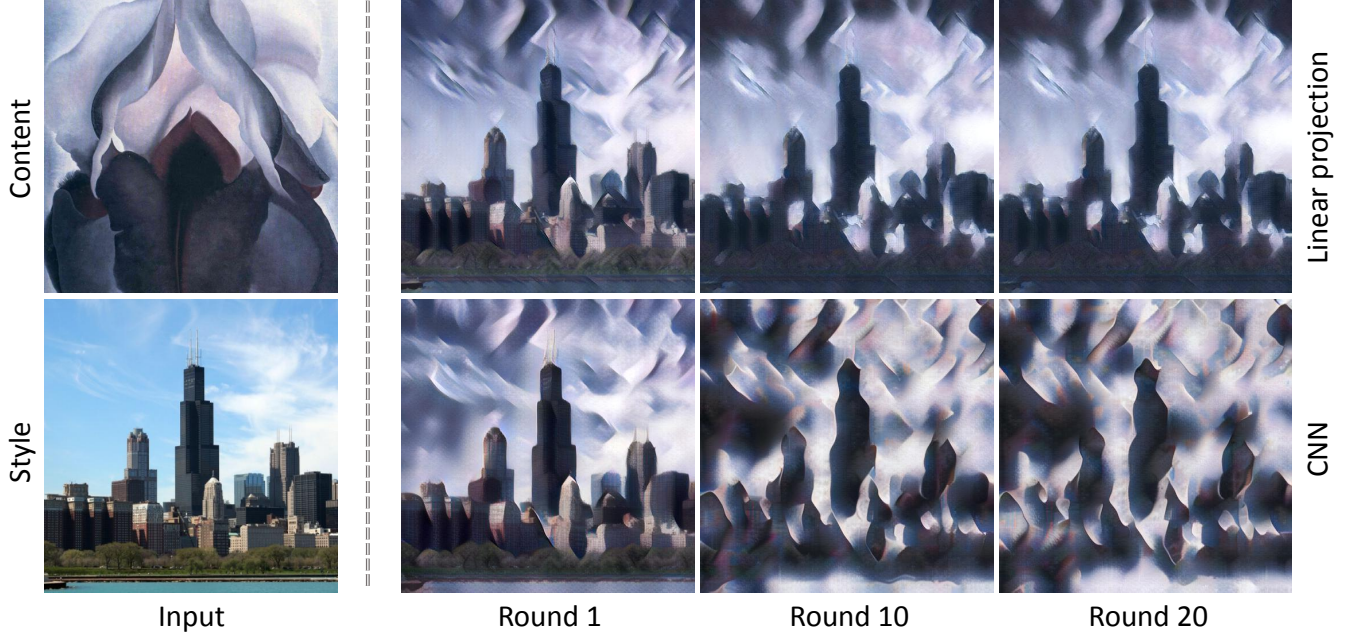


Fig. 12. Comparisons of CNN and Linear projection through several rounds of image stylization.

E. Timing Information

Our model is trained on 2 Tesla V100 and 2 GeForce RTX 3090 GPUs spending about one day. We compare the inference time of different style transfer methods using one piece of Tesla P100. Table IV shows the inference times of different methods using different scales of image size. Our method is faster than DFP, AAMS, and is comparable with ArtFlow.

F. Variance of Quantitative Evaluation

The quantitative evaluation is conducted by randomly selecting several content and style images. Therefore, we calculate the variance of content and style loss to show the random level. The statistics are shown in Table V. The content and style loss of

Output resolution	Ours	ArtFlow	MCC	DFP	AAMS	AdaIN
256×256	0.116	0.142	0.013	0.563	2.074	0.007
512×512	0.661	0.418	0.015	0.724	2.173	0.008

TABLE IV
INFERENCE TIME OF DIFFERENT METHODS (s).

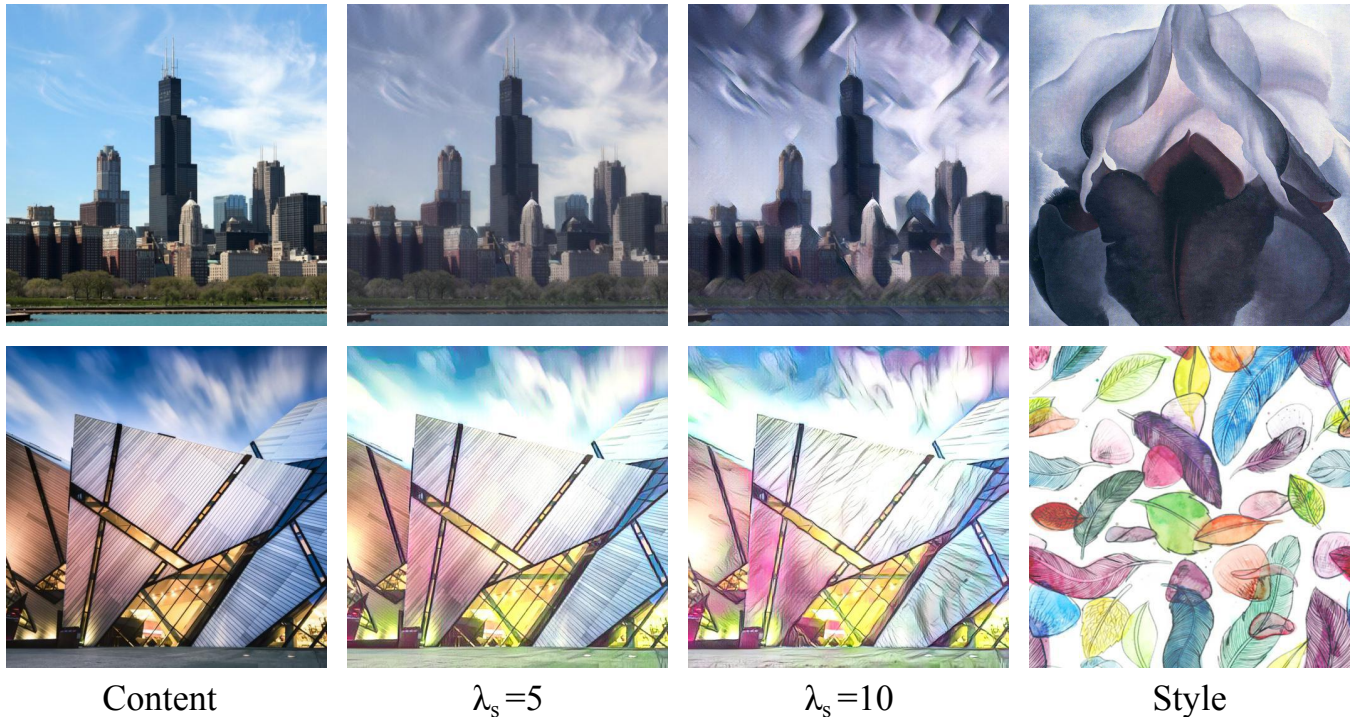


Fig. 13. Impact of style weight.

StyTr2 is lower than others with a small value float.

	Ours	ArtFlow	MCC	DFP	AAMS	AdaIN
\mathcal{L}_c	1.91 \pm 0.114	2.13 \pm 0.207	2.38 \pm 0.133	2.67 \pm 0.067	2.44 \pm 0.097	2.34 \pm 0.105
\mathcal{L}_s	1.47 \pm 0.950	3.08 \pm 1.800	1.56 \pm 0.972	2.12 \pm 1.652	3.18 \pm 2.070	1.91 \pm 1.760

TABLE V
VARIANCE OF QUANTITATIVE COMPARISONS.

G. Training Weight

The loss weights λ_c , λ_s , λ_{id1} , and λ_{id2} are adopted to eliminate the impact of magnitude differences. We change λ_s from 10 to 5 to survey the affect of style weight value. Figure 13 shows that reduction of style weight leads to less style patterns in generated results.

H. More Comparison Results

In this Section, we show more results to compare our method with AdaIN [6], AAMS [18], DFP [8], MCC [17] and ArtFlow [20].

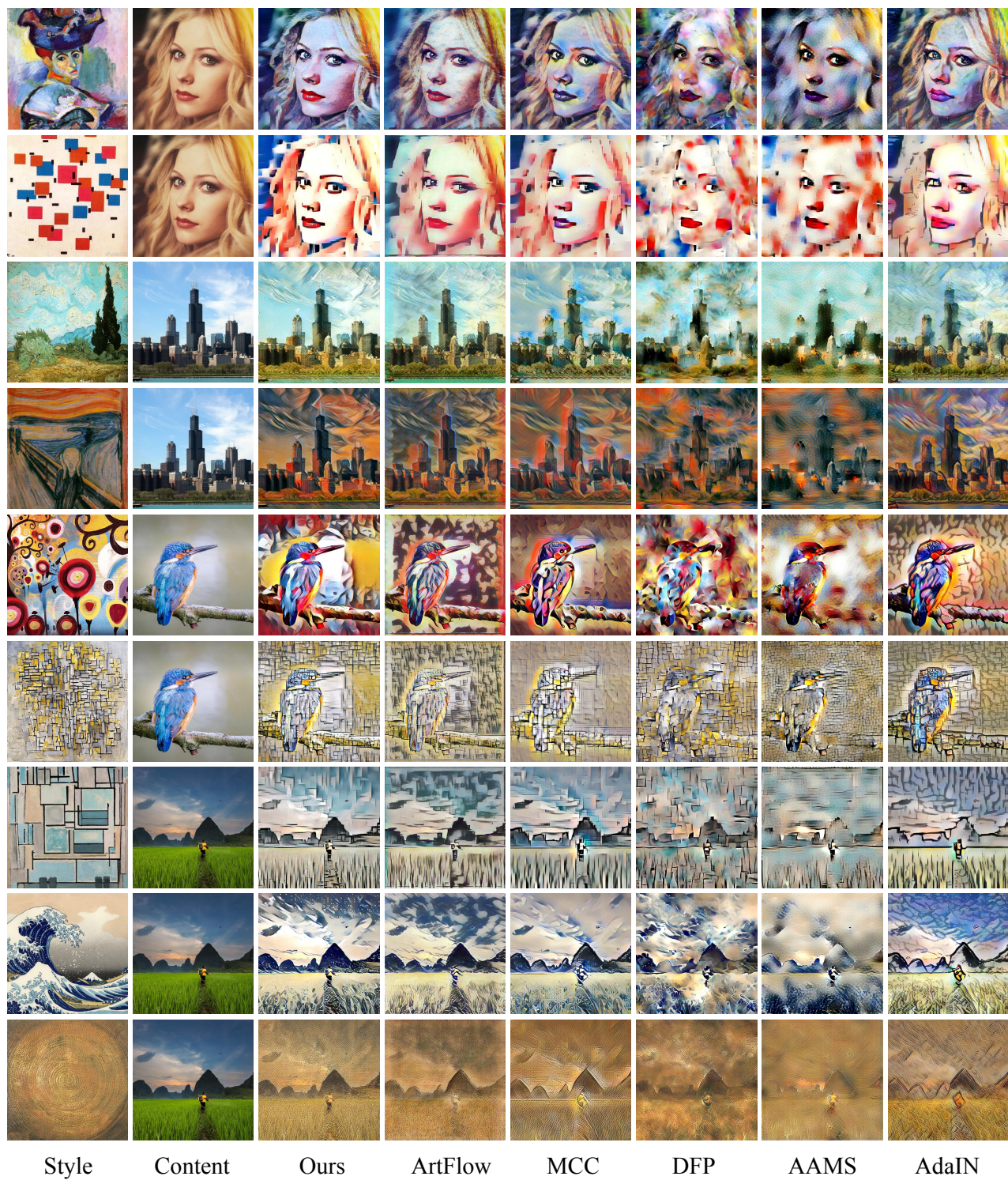


Fig. 14. Comparisons of different style transfer results. The first column shows style images, the second column shows content images. The remaining columns are stylized results.

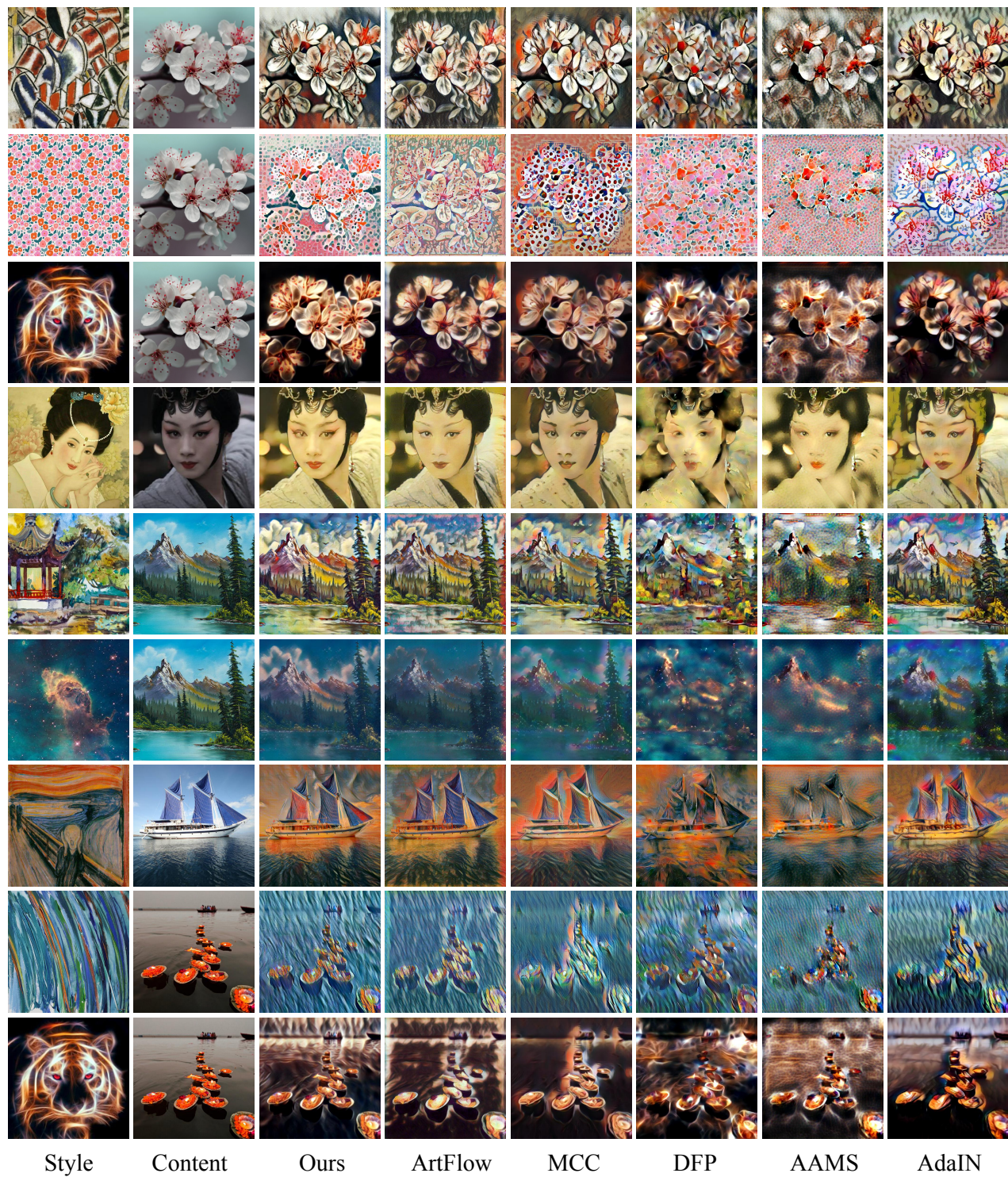


Fig. 15. Comparisons of different style transfer results. The first column shows style images, the second column shows content images. The remaining columns are stylized results.